

# PHYSICAL REVIEW B

## CONDENSED MATTER

THIRD SERIES, VOLUME 50, NUMBER 14

1 OCTOBER 1994-II

### Spectroscopic study and crystal-field analysis of $\text{Cm}^{3+}$ in the cubic-symmetry site of $\text{ThO}_2$

P. Thouvenot and S. Hubert

*Laboratoire de Radiochimie, Institut de Physique Nucleaire, Boite Postale No. 1, 91406 Orsay, France*

N. Edelstein

*Lawrence Berkeley Laboratory, Chemical Sciences Division, University of California, Berkeley, California 94720*

(Received 2 May 1994)

Fluorescence and excitation spectra of  $\text{Cm}^{3+}$  diluted in  $\text{ThO}_2$  powder are reported at room and low temperatures. The observed  $\text{Cm}^{3+}$  spectra are from the cubic symmetry lattice site and are assigned to phonon-assisted electric dipole transitions and to magnetic dipole transitions. From these assignments, the crystal-field parameters  $B_0^4 = -6436 \text{ cm}^{-1}$  and  $B_0^6 = 1195 \text{ cm}^{-1}$  have been determined. The experimental energy levels for the ground term ( $\sim 80\%$   $^8S_{7/2}$ ) determined from the optical data and earlier electron paramagnetic resonance spectra are in good agreement with the calculated values.

#### INTRODUCTION

$\text{Cm}$ , element number 96 in the Periodic Table, occurs in the center of actinide series and its trivalent ion,  $\text{Cm}^{3+}$  (radon core,  $5f^7$ ) has a half-filled shell. The differences in the electronic structure between the lanthanide counterpart  $\text{Gd}^{3+}$ ,  $4f^7$ , and  $\text{Cm}^{3+}$  demonstrate the effect of the much greater spin-orbit coupling that occurs in the  $5f$  series. The  $\text{Gd}^{3+}$  ground electronic term is an almost pure  $^8S_{7/2}$  configuration. Although this  $J=7/2$  ion splits in a crystalline field into at most four doublets, the total extent of the splitting is on the order of  $\sim 0.5 \text{ cm}^{-1}$ . The  $\text{Cm}^{3+}$  ion has a much larger spin-orbit coupling constant and its ground term is only  $\sim 80\%$   $^8S_{7/2}$ . As a consequence of the mixing of higher-lying states into the ground term by the spin-orbit coupling interaction (intermediate coupling), the ground-state splitting of the lowest  $J=7/2$  state of  $\text{Cm}^{3+}$  in solids is considerably larger than in  $\text{Gd}^{3+}$ ,  $\sim 2-50 \text{ cm}^{-1}$ .<sup>1</sup> The first correct report of the electron paramagnetic resonance (EPR) spectrum of  $\text{Cm}^{3+}$  was in  $\text{Cm}^{3+}/\text{LaCl}_3$  system, where the strongest resonance was assigned to a  $J_z = \frac{1}{2}$  level and assumed to be the ground state.<sup>2</sup> Carnall recently reanalyzed the available optical data on  $\text{Cm}^{3+}/\text{LaCl}_3$  and predicted a  $\mu = \frac{5}{2}$  level as the ground state in contradiction to the EPR data.<sup>3</sup> High-resolution optical measurements by Liu *et al.* on  $\text{Cm}^{3+}/\text{LaCl}_3$  show that the total splitting of the nominally  $^8S_{7/2}$  state in  $\text{LaCl}_3$  is  $1.97 \text{ cm}^{-1}$  and that the ground doublet is indeed a  $\mu = \frac{5}{2}$  level.<sup>4</sup> This doublet is EPR silent and with the ground term having a total splitting of  $1.97 \text{ cm}^{-1}$ , it was not possible to obtain

reliable intensity measurements as a function of temperature in the earlier EPR experiment.<sup>2</sup> Since the optical analysis of  $\text{Cm}^{3+}/\text{LaCl}_3$  gives a fit of  $\sigma = 20 \text{ cm}^{-1}$  [ $\sigma$  is the root-mean-square (rms) deviation] for 65 levels it may be fortuitous that in fact the parameters predict the correct doublet ground state, and indeed the correct ordering of the four doublets that comprise the ground term for a term that is split only by  $1.97 \text{ cm}^{-1}$ . Calculations predict a splitting of approximately  $\sim 7.5 \text{ cm}^{-1}$ .<sup>3</sup>

Similar results have been found in the  $\text{Cm}^{3+}/\text{LuPO}_4$  system. Here the total splitting of the ground term is  $12 \text{ cm}^{-1}$  from EPR measurements.<sup>5</sup> Analysis of the optical data is in progress, but the ordering of levels for the ground term is consistent with the EPR results.<sup>6</sup> EPR measurements of  $\text{Cm}^{3+}$  in cubic host materials such as the alkaline earth fluorides,  $\text{CeO}_2$ , and  $\text{ThO}_2$  show much larger zero-field splittings of the ground  $J = \frac{7}{2}$  term. Analyses of the spectra indicate total splittings of  $\sim 40 \text{ cm}^{-1}$  for  $\text{Cm}^{3+}/\text{CaF}_2$  and greater than  $15 \text{ cm}^{-1}$  for  $\text{Cm}^{3+}/\text{ThO}_2$ .<sup>1,7</sup>

In an earlier paper,<sup>8</sup> the analysis of the optical spectra of low concentrations of  $\text{Am}^{3+}$  ( $< 0.1\%$ ) diluted in powdered samples of  $\text{ThO}_2$ , showed optical spectra only from the trivalent  $5f^6$   $\text{Am}^{3+}$  ion at the cubic symmetry site assigned to magnetic dipole and phonon-assisted electric dipole transitions. Optical measurements on  $\text{Cm}^{3+}$  in  $\text{ThO}_2$  from selective excitation and fluorescence experiments are reported here and the crystal field parameters are derived from fitting these levels to an empirical Hamiltonian. These results are compared with other analyses of  $\text{Cm}^{3+}$  ions in various hosts.<sup>3-7</sup>

## EXPERIMENTAL PROCEDURE

The  $\text{ThO}_2$  sample doped with  $\text{Cm}^{3+}$  (0.05 at. %) was synthesized as a powder following the method described previously.<sup>8,9</sup> To avoid any fluorescence quenching due to radiation damage, the isotope  $^{248}\text{Cm}$  ( $\tau_{1/2}=3.4\times 10^5$  yr) was used which has a much lower specific activity than the more common  $^{244}\text{Cm}$  ( $\tau_{1/2}=18.1$  yr). The fluorescence and excitation spectra were recorded at room and liquid-helium temperatures and analyzed with a 1-m Jobin-Yvon monochromator with a dispersion of 8 Å/mm. The fluorescence was detected with a R636 Hamamatsu photomultiplier. The sample was placed in a liquid helium cryostat (Oxford Instruments) and excited with a Lambda-Physik dye laser (pulse length 76 ns and linewidth  $0.1\text{ cm}^{-1}$ ) pumped by a nitrogen laser. This experimental setup was controlled by a personal computer (PC).

The  $\text{Cm}^{3+}/\text{ThO}_2$  sample exhibited an intense red fluorescence under short-wavelength UV excitation (254 nm with a Hg lamp, or 337.1 nm with a  $\text{N}_2$  laser) at room and low temperature. Excitation spectra at room temperature and 10 K were obtained in the visible region by monitoring the emission line at 6260 Å. These spectra were obtained using several dyes (BBQ, BIS-MSB, DPS, Coumarin 440, 460, 480, 500, and Rhodamine 590 and 610).

## EXPERIMENTAL RESULTS AND ANALYSIS OF THE SPECTRA

In a crystal field of  $O_h$  symmetry, the crystal-field levels of trivalent curium are described by the group labels  $\Gamma_6$ ,  $\Gamma_7$ , and  $\Gamma_8$ , where  $\Gamma_6$  and  $\Gamma_7$  are each doubly degenerate and  $\Gamma_8$  is fourfold degenerate.<sup>10</sup> All the states will be referred to either by these labels and/or by the free-ion  $J$  states. In this symmetry the  $f$ - $f$  electric dipole transitions are forbidden, while the  $f$ - $f$  magnetic dipole transitions and the phonon-assisted electric dipole transitions are allowed. Thus, as was the case for  $\text{Am}^{3+}/\text{ThO}_2$ ,<sup>8</sup> strong, broad vibronic structure, as well as sharp magnetic dipole transitions, are observed.

### Fluorescence spectra

At room temperature the fluorescence spectrum exhibits a large band between 6000 and 6500 Å ( $15\,400$ – $16\,600\text{ cm}^{-1}$ ) (see Fig. 1) corresponding to the magnetic dipole transition from the first excited state ( ${}^6D_{7/2}$ ,  ${}^6P_{5/2}$ ) to the  ${}^8S_{7/2}$  ground state. The structure observed on each side of the intense line at  $15\,969\text{ cm}^{-1}$  is attributed to vibronic transitions located at the energies differences corresponding to the vibronic modes of the matrix (97, 276, 356, 475, and  $575\text{ cm}^{-1}$ ) and are assigned to the IR active modes.<sup>8,9</sup> As shown in Fig. 1, the emission spectrum at  $\sim 10\text{ K}$  is due primarily to a doublet at 15 984 and  $15\,969\text{ cm}^{-1}$ . These narrow lines correspond to magnetic dipole transitions coming from the first optically excited state at  $15\,984\text{ cm}^{-1}$  to the  ${}^8S_{7/2}$  ground state and to the second crystal-field level at  $15\text{ cm}^{-1}$ . The vibronic structure situated on the high-energy side at room temperature disap-

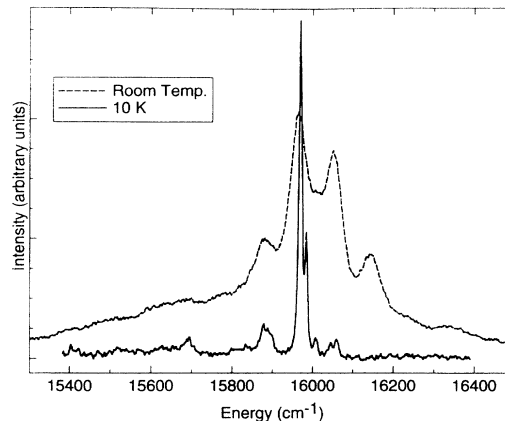


FIG. 1. Room-temperature and low-temperature fluorescence of  $\text{Cm}^{3+}/\text{ThO}_2$ .

pears at low temperature. The  $\text{Cm}^{3+}/\text{ThO}_2$  sample exhibits an intense red fluorescence under short-wavelength UV excitation at room and low temperatures. On the low-energy side of the strong fluorescence a weak band at  $15\,878\text{ cm}^{-1}$  is observed, which is located at  $91\text{ cm}^{-1}$  from the zero phonon line and corresponds to a vibronic line. The assigned emission lines observed at 10 K are presented in Table I. Note that the transition from the  ${}^6D_{7/2}$  excited level to the third crystal field level of the ground  ${}^8S_{7/2}$  term is not observed in the emission spectrum.

### Excitation spectra

The excitation spectra obtained in the visible region at  $\sim 10\text{ K}$  are shown in Figs. 2 and 3. Numerous vibronic lines associated either with magnetic dipole transitions or with absent electric dipole transitions are observed. In the latter case, the assignments of the vibronic bands determine the energies of the forbidden 0-0 transitions. However unlike  $\text{Am}^{3+}/\text{ThO}_2$ , many narrow lines from magnetic dipole transitions also were observed. The spectra are assigned on the basis of the  $\text{Cm}^{3+}$  ions occupying only a cubic symmetry site in agreement with the data for  $\text{Am}^{3+}/\text{ThO}_2$ .<sup>8</sup>

TABLE I. Zero-phonon and phonon-assisted transitions energies from the luminescence spectrum at 10 K.

Wavelength $\lambda(\text{Å})$	Energy ( $\text{cm}^{-1}$ )	Transitions	$\Delta E^a$ ( $\text{cm}^{-1}$ )	$\Delta E^b$ ( $\text{cm}^{-1}$ )
6225	16 060		91	
6254.5	15 984	${}^6D_{7/2} \rightarrow {}^8S_{7/2}$	0	0
6260.5	15 969	${}^6D_{7/2} \rightarrow {}^8S_{7/2}$	0	15
6290.5	15 893		90	
6369	15 695		274	
6445	15 512		457	
6489	15 407		562	

<sup>a</sup>Energy differences between the zero-phonon transition and phonon-assisted transitions.

<sup>b</sup>Energy differences between the Stark levels of the  ${}^8S_{7/2}$  ground state.

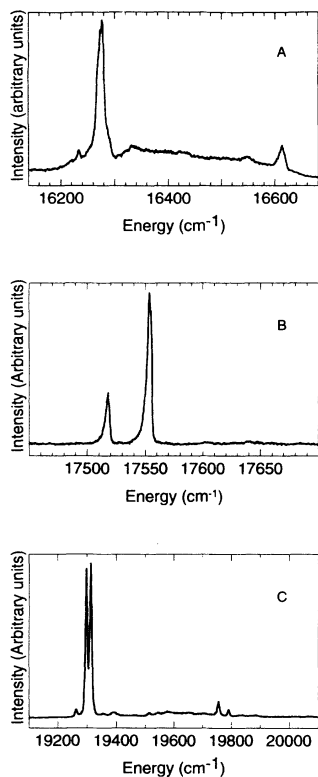


FIG. 2. Excitation spectra of  $\text{Cm}^{3+}/\text{ThO}_2$  at 10 K. (a) 16 100–16 700  $\text{cm}^{-1}$  region (b) 17 400–17 700  $\text{cm}^{-1}$  region showing the crystal-field splitting between the first (lowest) and the third crystal-field level of the ground term; (c) 19 100–20 000  $\text{cm}^{-1}$  region showing the splitting between the first and second crystal-field levels of the ground term ( $\sim 19\,300\text{ cm}^{-1}$ ) as well as the splitting between the first and third levels ( $\sim 19\,790\text{ cm}^{-1}$ ).

Although only the lowest component of the  ${}^6D_{7/2}$  is found in the luminescence spectra at  $15\,984\text{ cm}^{-1}$ , in the excitation spectrum between  $16\,100$  and  $16\,700\text{ cm}^{-1}$ , the second Stark level of the  ${}^6D_{7/2}$  multiplet is observed at  $16\,277\text{ cm}^{-1}$ , Fig. 2(a). The third  ${}^6D_{7/2}$  crystal-field component appears in the region between  $17\,400$  and  $17\,700\text{ cm}^{-1}$ . At 10 K, the two narrow lines at  $17\,518$  and  $17\,554\text{ cm}^{-1}$  correspond to transitions arising from the second excited level of the ground term at  $36\text{ cm}^{-1}$  and from the  ${}^8S_{7/2}$  ground state to the third Stark component of the  ${}^6D_{7/2}$  term, Fig. 2(b). In the excitation spectrum between  $19\,100$  and  $20\,000\text{ cm}^{-1}$ , two narrow doublets correspond to transitions coming from the  ${}^8S_{7/2}$  ground state and the  $15\text{ cm}^{-1}$  level to the  ${}^6P_{5/2}$  state at  $19\,315\text{ cm}^{-1}$ , and from the ground state and the  $35\text{ cm}^{-1}$  level to the  ${}^6P_{5/2}$  level at  $19\,791\text{ cm}^{-1}$ ; see Fig. 2(c). The weak feature at  $19\,263\text{ cm}^{-1}$  is unassigned.

In the region from  $20\,660$  to  $26\,500\text{ cm}^{-1}$  (Fig. 3), the excitation spectra become more complicated. Most of the features observed can be assigned to intense vibronic transitions associated with electric dipole transitions and to a few narrow lines associated with zero-phonon magnetic dipole transitions. As in the analysis of the optical spectra of  $\text{Am}^{3+}/\text{ThO}_2$ ,<sup>8</sup> the zero-phonon electric dipole transitions can be deduced from the vibronic assign-

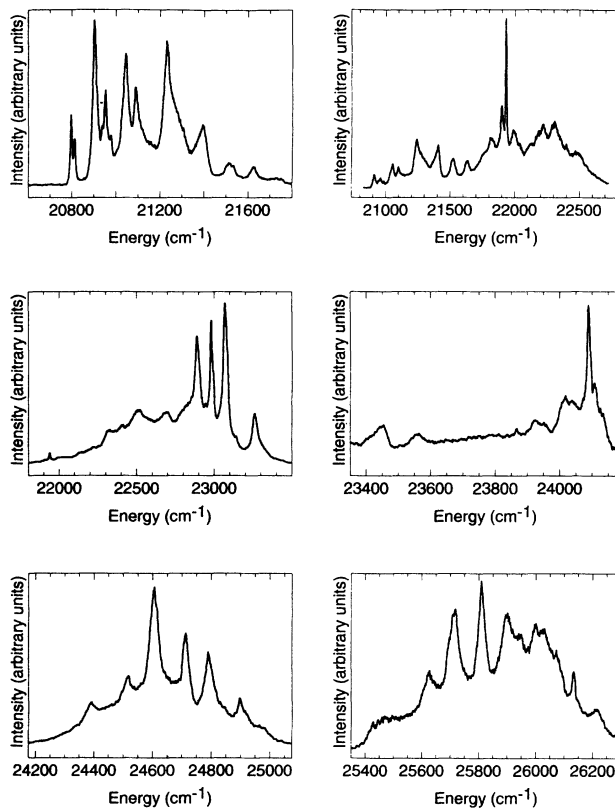


FIG. 3. Excitation spectra of  $\text{Cm}^{3+}/\text{ThO}_2$  at 10 K between  $20\,600$  and  $26\,300\text{ cm}^{-1}$ .

ments. Table II lists the energies of the zero-phonon transitions with their associated vibronic lines. Sixteen excited states were assigned. The transitions involving the  ${}^8S_{7/2}$  ground manifold allow the determination of the total splitting of the ground state. From the emission and excitation spectra, the crystal-field splittings of the ground manifold are determined to be  $0$ ,  $15$ , and  $36\text{ cm}^{-1}$ .

## DISCUSSION

The levels were fit by simultaneous diagonalization of the free-ion ( $H_{\text{FI}}$ ) and crystal-field ( $H_{\text{CF}}$ ) Hamiltonians:

$$H_{\text{FI}} = \sum_{k=0,2,4,6} F^k(nf, nf) f_k + \zeta_f \alpha_{\text{s.o.}} + \alpha L(L+1) \\ + \beta G(G_2) + \gamma(R_7) + \sum_{\substack{k=2,8 \\ k \neq 5}} T^k t_k \\ + \sum_{k=0,2,4} M^k m_k + \sum_{k=2,4,6} P^k p_k$$

and

$$H_{\text{CF}} = B_0^4 [C_0^4 + (5/14)^{1/2} (C_{-4}^4 + C_4^4)] \\ + B_0^6 [C_0^6 - (7/2)^{1/2} (C_{-4}^6 + C_4^6)].$$

The  $F^k(nf, nf)$  and  $\zeta_f$  parameters above represent the radial part of the electrostatic interaction between two  $f$  electrons, and the spin-orbit interaction, respectively, while  $f_k$  and  $\alpha_{\text{s.o.}}$  are angular parts of these interactions. The parameters  $\alpha, \beta, \gamma$  are associated with the two-body

TABLE II. Energies of zero-phonon and phonon-assisted transitions from excitation spectra at 10 K.

Wavelength $\lambda$ (Å)	Energy (cm <sup>-1</sup> )	Transitions <sup>8</sup> S <sub>7/2</sub> →	$\Delta E^a$ (cm <sup>-1</sup> )	$\Delta E^b$ (cm <sup>-1</sup> )	Wavelength $\lambda$ (Å)	Energy (cm <sup>-1</sup> )	Transitions <sup>8</sup> S <sub>7/2</sub> →	$\Delta E^a$ (cm <sup>-1</sup> )	$\Delta E^b$ (cm <sup>-1</sup> )
6142	16 277	<sup>6</sup> D <sub>7/2</sub>		11	4333	23 073		91	
6138	16 288	<sup>6</sup> D <sub>7/2</sub>	0		4297.5	23 263		281	
5707	17 518	<sup>6</sup> D <sub>7/2</sub>		36	4265	23 440		458	
5695	17 554	<sup>6</sup> D <sub>7/2</sub>	0		4243	23 562		580	
5190	19 263			52 <sup>c</sup>	(4198)	(23 815)	<sup>6</sup> I <sub>11/2</sub>	0	
5180	19 300	<sup>6</sup> P <sub>5/2</sub>		15	4181	23 912		97	
5176	19 315	<sup>6</sup> P <sub>5/2</sub>	0		4150	24 090		275	
5060.5	19 756	<sup>6</sup> P <sub>5/2</sub>	0	35	(4176)	(23 940)	<sup>4</sup> I <sub>17/2</sub>	0	
5051.5	19 791	<sup>6</sup> P <sub>5/2</sub>	0		4159	24 036		97	
4807	20 797	<sup>6</sup> I <sub>7/2</sub>		15	4128.5	24 215		275	
4803.5	20 812	<sup>6</sup> I <sub>7/2</sub>	0		4099	24 390		450	
4783	20 902		90		4078	24 516		576	
4740	21 090		278		(4109)	(24 330)	<sup>4</sup> I <sub>17/2</sub>	0	
4675	21 383		571		4063.5	24 603		273	
4774.5	20 939	<sup>6</sup> I <sub>7/2</sub>		17	4033	24 789		459	
4770.5	20 956	<sup>6</sup> I <sub>7/2</sub>	0		4015	24 901		571	
4749	21 051		95		4046	24 710	<sup>6</sup> D <sub>9/2</sub>	0	
4709	21 230		274		(3943)	(25 353)	<sup>6</sup> I <sub>13/2</sub>	0	
4669	21 412		456		3901	25 628		275	
4643	21 532		576		3888	25 710		357	
4599	21 738	<sup>6</sup> I <sub>7/2</sub>	0		3873.5	25 808		455	
4581	21 823		93		3853	25 946		593	
4544	22 001		271		(3929)	(25 444)	<sup>6</sup> I <sub>13/2</sub>	0	
4504	22 196		466		3887	25 718		274	
4483	22 300		570		3873.5	25 808		365	
4565.5	21 897	<sup>6</sup> I <sub>9/2</sub>		36	3860	25 900		456	
4558	21 933	<sup>6</sup> I <sub>9/2</sub>	0		3840	26 034		591	
4538	22 030		97		(3902)	(25 620) <sup>c,e</sup>		0	
4505	22 203		270		3887	25 718		98	
4464.5	22 405		464		3860	25 899		279	
4442	22 506		573		3834	26 074		454	
4367	22 890		92		3816	26 195		575	
4357	22 946	<sup>6</sup> I <sub>9/2</sub>		36	3825.5	26 132	<sup>6</sup> D <sub>9/2</sub>	0	
4350	22 982	<sup>6</sup> I <sub>9/2</sub>	0		3813	26 218		84	
4347	22 997 <sup>d</sup>								

<sup>a</sup>Energy differences between the zero-phonon line and vibronic lines.

<sup>b</sup>Energy differences between the <sup>8</sup>S<sub>7/2</sub> ground-state multiplets.

<sup>c</sup>Not assigned.

<sup>d</sup>Shoulder, not assigned.

<sup>e</sup>Not used in the fitting procedure.

effective operators of the configuration interaction, and the  $T^k$ 's are the corresponding parameters of the three-body configuration interaction operators. The  $M^k$  parameters represent the spin-spin and spin-orbit interactions, and the  $P^k$  parameters arise from electrostatic-spin-orbit interactions with higher configurations. For  $O_h$  symmetry the crystal-field interaction is parametrized by  $B_0^4$  and  $B_0^6$  and the angular operators of  $C_q^k$  are the Racah tensors.<sup>11</sup>

The crystal-field parameters obtained earlier for  $\text{Am}^{3+}/\text{ThO}_2$ ,<sup>8</sup> and the  $\text{Cm}^{3+}/\text{LaCl}_3$  free-ion parameters found by Carnall,<sup>3</sup> were used initially for fitting the experimental levels. For the first fit, the crystal-field parameters were held fixed, and  $F^2$ ,  $F^4$ ,  $F^6$ , and  $\zeta$  were allowed to vary freely using 11 experimental levels. Then the four free-ion parameters were fixed at the values that gave the minimum rms deviation between the calculated

and experimental energy levels, and the crystal-field parameters were varied. Further energy levels were assigned and finally the above four free-ion parameters and the two crystal-field parameters were varied simultaneously. The results of the fits and the final assignments of the experimental and calculated levels are given in Table III. The  $O_h$  symmetry labels were assigned on the basis of the calculated energy levels and wave functions. In the final fit 20 experimental levels were used and a rms deviation of 21.7 cm<sup>-1</sup> was obtained. One experimental level from Table III (25 620 cm<sup>-1</sup>) was not used in the fit as it gave a much greater deviation than any other level. The calculated ground-state  $g$  value of 4.513 is in good agreement with the experimental EPR  $g$  value of 4.484.

The crystal-field states of the ground manifold show good agreement between the calculated and experimental levels. The ground state is a  $\Gamma_6$  level and the energy of

the first excited state ( $\Gamma_8$ ) is in agreement with the value obtained from EPR data. The energy splitting of  $15.5 \pm 0.3 \text{ cm}^{-1}$  was determined from the magnitude of the anisotropy of the  $g$  value of the ground  $\Gamma_6$  state caused by the magnetic-field mixing between the  $\Gamma_6$ - $\Gamma_8$  states.<sup>7</sup> As pointed out by Edelstein and Easley,<sup>1</sup> Carnall,<sup>3</sup> and Liu, Beitz, and Huang,<sup>4</sup> the substantially increased spin-orbit coupling and reduced electrostatic interaction for  $5f$  electrons results in a higher degree of admixture of excited states into the ground state when compared to  $\text{Gd}^{3+}$ . In this work the ground-state wave function for  $\text{Cm}^{3+}$  is approximately 78%  $^8S_{7/2}$  and 19%  $^6P_{7/2}$ . The empirical parameters found for  $\text{Cm}^{3+}/\text{ThO}_2$  are given in Table IV and compared with the parameters

TABLE III. Calculated and experimental energy levels for  $\text{Cm}^{3+}/\text{ThO}_2$ .

Level	Largest $S$ - $L$ - $J$ Comp.	Calc. energy ( $\text{cm}^{-1}$ )	Expt. energy ( $\text{cm}^{-1}$ )	$\Delta(E_{\text{expt.}} - E_{\text{calc.}})$ ( $\text{cm}^{-1}$ )
$1\Gamma_6$	$^8S_{7/2}$	-1.7	0	1.7
$1\Gamma_8$	$^8S_{7/2}$	10.8	15	4.2
$1\Gamma_7$	$^8S_{7/2}$	40.8	36	-4.8
$2\Gamma_6$	$^6D_{7/2}$	16025.9	15984	-41.9
$2\Gamma_8$	$^6D_{7/2}$	16255.0	16288	33.0
$2\Gamma_7$	$^6D_{7/2}$	17568.7	17554	-14.7
$3\Gamma_8$	$^6P_{5/2}$	19314.2	19315	0.8
$3\Gamma_7$	$^6P_{5/2}$	19792.7	19791	-1.7
$3\Gamma_6$	$^6I_{7/2}$	20831.4	20812	-19.4
$4\Gamma_8$	$^6I_{7/2}$	20938.9	20956	17.1
$5\Gamma_8$	$^6P_{3/2}$	21450.3		
$4\Gamma_7$	$^6I_{7/2}$	21709.0	21738	29.0
$4\Gamma_6$	$^6I_{9/2}$	21910.0	21933	23.0
$6\Gamma_8$	$^6I_{9/2}$	22097.2		
$7\Gamma_8$	$^6I_{9/2}$	22973.3	22982	8.7
$5\Gamma_7$	$^6I_{11/2}$	23689.9		
$8\Gamma_8$	$^6I_{11/2}$	23818.4	23815	-3.4
$9\Gamma_8$	$^6I_{17/2}$	23940.5	23940	-0.5
$5\Gamma_6$	$^6I_{17/2}$	24034.5		
$10\Gamma_8$	$^6I_{17/2}$	24089.2		
$11\Gamma_8$	$^6I_{17/2}$	24289.1		
$6\Gamma_6$	$^6I_{17/2}$	24340.3	24330	-10.3
$6\Gamma_7$	$^6I_{17/2}$	24374.6		
$12\Gamma_8$	$^6I_{17/2}$	24669.8		
$13\Gamma_8$	$^6I_{17/2}$	24729.8	24710	-19.8
$7\Gamma_7$	$^6I_{13/2}$	24847.6		
$7\Gamma_6$	$^6I_{11/2}$	24868.4		
$14\Gamma_8$	$^6I_{13/2}$	24976.6		
$8\Gamma_6$	$^6I_{15/2}$	25184.0		
$15\Gamma_8$	$^6I_{15/2}$	25288.6		
$8\Gamma_7$	$^6I_{13/2}$	25305.7		
$9\Gamma_6$	$^6I_{13/2}$	25329.0		
$9\Gamma_7$	$^6I_{13/2}$	25346.9	25353	6.1
$16\Gamma_8$	$^6I_{13/2}$	25434.9	25444	9.1
$17\Gamma_8$	$^6I_{15/2}$	25773.5		
$18\Gamma_8$	$^6I_{15/2}$	25906.3		
$10\Gamma_6$	$^6D_{9/2}$	26148.1	26132	-16.1
$19\Gamma_8$	$^6D_{9/2}$	26195.8		
$10\Gamma_7$	$^6D_{7/2}$	27149.4		
$11\Gamma_6$	$^6D_{7/2}$	27489.8		
$20\Gamma_8$	$^6D_{7/2}$	27502.9		

for  $\text{Am}^{3+}/\text{ThO}_2$ .<sup>8</sup> As expected, the crystal-field parameters of the  $\text{Cm}^{3+}$  ion ( $5f^7$ ) in  $\text{ThO}_2$  are almost the same as for  $\text{Am}^{3+}$  ( $5f^6$ ). The value of  $B_0^4$  parameter is slightly smaller than it is for  $\text{Am}^{3+}$ , the  $B_0^6$  is rather larger. However, the crystal-field strength parameter  $N'_y$  defined elsewhere<sup>8</sup> gives almost the same value for  $\text{Cm}^{3+}$  ( $2951 \text{ cm}^{-1}$ ) as for  $\text{Am}^{3+}$  ( $2945 \text{ cm}^{-1}$ ), as expected for ions that are neighbors in the Periodic Table.

In the emission spectrum, only two magnetic dipole transitions are observed. They originate from the first excited level at  $15984 \text{ cm}^{-1}$  to the first two components of the  $^8S_{7/2}$  ground state at 0 and  $15 \text{ cm}^{-1}$ . A third transition from the  $15984 \text{ cm}^{-1}$  level terminating at the third excited level ( $\Gamma_7$ ) above the ground state was not observed in the fluorescence spectrum. Magnetic dipole intensity calculations for the transitions give the calculated intensities  $1.58 \times 10^{-3}$  and  $4.8 \times 10^{-3}$  for the transitions from the emitting state to the first two states of the ground manifold and  $2.74 \times 10^{-17}$  for the transition to the third state. Moreover the relative intensity of these two observed magnetic dipole transitions have approximately the same ratio as that calculated.

It is interesting to note that in all cases where an optical analysis of  $\text{Cm}^{3+}$  in a host matrix has been reported, the splittings predicted from the analysis reproduce the correct ordering of the states in the ground  $\sim^8S_{7/2}$  term.<sup>3,4,6</sup> However in the present work the magnitudes of the splittings are approximately reproduced by the crystal-field parameters. For  $\text{Cm}^{3+}/\text{ThO}_2$  the total ground-state splitting is  $36 \text{ cm}^{-1}$  as compared to a maximum of  $\sim 12 \text{ cm}^{-1}$  for the other hosts, where all levels

TABLE IV. Values of the spectroscopic parameters.

Parameters	$\text{Am}^{3+}/\text{ThO}_2^a$ ( $\text{cm}^{-1}$ )	$\text{Cm}^{3+}/\text{ThO}_2^b$ ( $\text{cm}^{-1}$ )
$F^2$	48038.0(140.2)	50523.6(102.4)
$F^4$	39684.2(212.9)	47933.9(130.2)
$F^6$	29574.1(171.4)	29271.3(83.8)
$\zeta$	2511.1(27.0)	2691.1(14.1)
$\alpha$	33.2(8.6)	[28.3]
$\beta$	[-660]	[-650]
$\gamma$	[1000]	[825]
$T^2$	[200]	[200]
$T^3$	[50]	[50]
$T^4$	[40]	[40]
$T^6$	[-360]	[-360]
$T^7$	[390]	[390]
$T^8$	[340]	[340]
$M^0$	[0.99]	[1.09]
$M^2$	[0.55]	[0.61]
$M^4$	[0.38]	[0.41]
$P^2$	[850]	[912]
$P^4$	[637.5]	[684]
$P^6$	[425]	[456]
$B_0^4$	-6731.32(96.0)	-6446.5(42.6)
$B_0^6$	713.6(115.0)	1142.1(32.1)

<sup>a</sup>From Ref. 8. All parameters values in [ ] held fixed in the fitting procedure.

<sup>b</sup>20 experimental levels, rms deviation  $21.7 \text{ cm}^{-1}$ .

have been measured. In  $\text{ThO}_2$  the crystal field is large enough so that the  $\text{Cm}^{3+}$  ground-state splittings due to intermediate coupling effects are dominant over other splitting mechanisms. Thus the conventional crystal-field model can reproduce the observed splittings of the ground state and the excited states in a satisfactory way.

### CONCLUSION

The fluorescence and excitation spectra of  $\text{Cm}^{3+}$  have been assigned. The crystal-field parameters were obtained by fitting the 20 levels deduced either from magnetic dipole transitions or from phonon-assisted electric dipole transitions. The optical data for the ground-state splittings are in very good agreement with levels obtained earlier from EPR measurements. While the fourth-order crystal-field parameter  $B_0^4$  is almost the same as found for

$\text{Am}^{3+}$ , the sixth-order parameter is larger for  $\text{Cm}^{3+}$  than  $\text{Am}^{3+}$ . However, the magnitude of the sixth-order parameter is still much smaller than that found from neutron-diffraction experiments on the  $\text{UO}_2$ ,  $\text{NpO}_2$  and  $\text{PuO}_2$ .<sup>8</sup>

### ACKNOWLEDGMENTS

This research was sponsored in part by the Director, Office of Energy Research, Office of Basic Energy Sciences, Chemical Sciences Division of the U.S. Department of Energy under Contract No. DE-AC03-76SF00098. The authors are indebted, for the use of  $^{248}\text{Cm}$ , to the Division of Chemical Sciences, Office of Basic Energy Sciences, through the transplutonium element production facilities at Oak Ridge National Laboratory.

---

<sup>1</sup>N. Edelstein and W. Easley, *J. Chem. Phys.* **48**, 2110 (1968).

<sup>2</sup>M. M. Abraham, B. R. Judd, and H. Wickman, *Phys. Rev.* **130**, 611 (1963).

<sup>3</sup>W. T. Carnall, *J. Chem. Phys.* **96**, 8713 (1992).

<sup>4</sup>G. K. Lui, J. V. Beitz, and J. Huang, *J. Chem. Phys.* **99**, 3304 (1993).

<sup>5</sup>W. K. Kot, N. Edelstein, M. M. Abraham, and L. A. Boatner, *Phys. Rev. B* **48**, 12 704 (1993).

<sup>6</sup>J. Systma, N. Edelstein, M. M. Abraham, and L. A. Boatner (unpublished).

<sup>7</sup>W. Kolbe, N. Edelstein, C. B. Finch, and M. M. Abraham, *J.*

*Chem. Phys.* **56**, 5432 (1972); *J. Chem. Phys.* **58**, 820 (1973).

<sup>8</sup>S. Hubert, P. Thouvenot, and N. Edelstein, *Phys. Rev. B* **48**, 5751 (1993).

<sup>9</sup>S. Hubert and P. Thouvenot, *J. Luminesc.* **54**, 103 (1992).

<sup>10</sup>G. F. Koster, J. O. Dinnock, R. G. Wheeler, and H. Statz, *Properties of the Thirty-Two Point Groups* (MIT Press, Cambridge, MA, 1963).

<sup>11</sup>W. T. Carnall, H. Crosswhite, H. M. Crosswhite, J. P. Hessler, N. M. Edelstein, J. G. Conway, G. V. Shalimoff, and R. Sarup, *J. Chem. Phys.* **72**, 5089 (1980).